AGU PUBLICATIONS

Geophysical Research Letters

RESEARCH LETTER
10.1002/2016GL067964

Key Points:
- Idealized AGCM responses to polar stratospheric cooling studied
- Responses to imposed ozone depletion-like cooling sensitive to timing of cooling
- Responses involve the second EOF as well as the first

Supporting Information:
- Supporting Information S1

Correspondence to:
A. Sheshadri,
as4915@columbia.edu

Citation:
Sheshadri, A., and R. A. Plumb (2016), Sensitivity of the surface responses of an idealized AGCM to the timing of imposed ozone depletion-like polar stratospheric cooling, *Geophys. Res. Lett.*, *43*, doi:10.1002/2016GL067964.

Received 27 JAN 2016
Accepted 26 FEB 2016
Accepted article online 2 MAR 2016

Sensitivity of the surface responses of an idealized AGCM to the timing of imposed ozone depletion-like polar stratospheric cooling

Aditi Sheshadri[1,2] and R. Alan Plumb[1]

[1]Department of Earth, Atmospheric, and Planetary Sciences, Massachusetts Institute of Technology, Cambridge, Massachusetts, USA, [2]Now at Department of Applied Physics and Applied Mathematics, Columbia University, New York, New York, USA

Abstract An idealized atmospheric general circulation model (AGCM) is used to investigate the sensitivity of model responses to the timing of imposed polar stratospheric cooling, intended to mimic the radiative effects of ozone depletion. The model exhibits circulation responses to springtime cooling that qualitatively match both observations and the responses of comprehensive chemistry climate models. The model's surface response is sensitive to the timing of the cooling, with the onset becoming delayed with later cooling, but with the termination occurring at similar times, suggesting that the meteorology plays an important role. The model's responses do not match the latitudinal structure of the leading annular mode; rather, the response described by the second empirical orthogonal function plays a substantial role, in addition to the first. It is suggested that the imposed cooling, when it delays the final warming, results in an extended period of lower stratospheric variability, which could be an important factor in producing realistic surface responses.

1. Introduction

Polar stratospheric ozone depletion is widely regarded as the primary driver of tropospheric circulation changes in austral summer over the second half of the twentieth century [e.g., *Polvani et al.*, 2011, *Thompson et al.*, 2011]. These changes are usually described as an increase in the positive phase of the Southern Annular Mode (SAM), i.e., an increase in zonal mean sea level pressure difference between the middle and high latitudes [e.g., *Thompson et al.*, 2000; *Fogt et al.*, 2009]. The positive phase of the SAM is associated with a poleward shift of the Southern Hemisphere midlatitude jet and storm tracks [*Archer and Caldeira*, 2008]. Ozone depletion has also been associated with an observed seasonal poleward expansion of the Hadley cell [*Hu and Fu*, 2007].

The polar stratospheric cooling that is a consequence of ozone depletion is largest during austral spring (September-October-November), following the season of maximum ozone depletion [e.g., *Previdi and Polvani*, 2014]. In the years prior to the development of the ozone hole, the seasonal breakdown of the Antarctic stratospheric polar vortex (the "final warming") was observed to occur on the average in early to middle November. Spring cooling of the polar stratosphere by ozone depletion, through thermal wind balance, strengthens the Antarctic polar vortex toward the end of its lifetime and extends the persistence of the polar vortex; i.e., it delays the final warming [*Waugh et al.*, 1999; *Black and McDaniel*, 2007b; *Sheshadri et al.*, 2014; *Sun et al.*, 2014], which is observed to occur in early December in the years of large ozone depletion. These changes in the stratospheric circulation have been regarded as being dynamically coupled to the tropospheric circulation changes in austral summer (December-January-February); that is, the tropospheric circulation changes lag the stratospheric ones by 1–2 months [*Previdi and Polvani*, 2014]. Model studies in which stratospheric ozone depletion is imposed either directly or by changing emissions of ozone-depleting substances support this conclusion [e.g., *Sigmond et al.*, 2010, *Polvani et al.*, 2011, *McLandress et al.*, 2011].

Sun et al. [2014] reported that in their idealized model, surface wind trends resembling those observed are not evident in years in which the stratospheric final warming is not delayed. *Sigmond and Fyfe* [2014] showed that models forced with observed ozone depletion agree on the sign but not the magnitude of their annular mode response to imposed ozone depletion. *Wilcox and Charlton-Perez* [2013] show that a common bias among CMIP5 models is that the date of their Antarctic polar vortex breakdown in runs with observed radiative forcings is approximately two weeks later than observed values for the years 1980–1999. This bias, coupled with the findings of *Sun et al.* [2014], raises the question of how sensitive a model's responses are

to the timing of imposed ozone depletion relative to the model's final warming date. In other words, if the imposed ozone depletion does not cause a delay in the model's final warming (i.e., if there is a gap between the imposed ozone depletion and the final warming date, because the model's own final warming is delayed relative to observations), is the model missing some of the response to the radiative forcing of ozone depletion?

To address this issue, we study the responses of an idealized atmospheric general circulation model to polar stratospheric cooling that is meant to mimic the radiative impacts of polar stratospheric ozone depletion but imposed at different phases of the lifetime of the vortex. Section 2 contains a brief model description, as well as a description of the imposed polar stratospheric cooling. In section 3, we demonstrate that the model's surface responses to polar stratospheric cooling imposed in austral spring qualitatively match observations. We then present the model's responses to polar stratospheric cooling imposed at different stages of the vortex's lifetime. We find some sensitivity to the timing of imposed polar stratospheric cooling, with the onset of the response being delayed as the timing of the imposed cooling is delayed but the termination of the response occurring at approximately similar times. In addition, we examine the model's response to steady (all-year) cooling. Interestingly, both with seasonal and all-year cooling, we find that the model's response does not match the latitudinal structure of the model's leading annular mode at certain times of the year, with the mismatch being greatest in austral spring. A summary is presented in section 4.

2. Model Setup

The model setup is based on that of *Polvani and Kushner* [2002] and is almost identical to that of *Sheshadri et al.* [2015]. The model is dry and hydrostatic, solving the global primitive equations with T42 resolution in the horizontal and 40 σ levels in the vertical. There is no bottom topography. Radiation and convection schemes are replaced by relaxation to a zonally symmetric equilibrium temperature profile that in the troposphere is similar to that of Held and Suarez, with a tropospheric asymmetry parameter ε [as in *Polvani and Kushner*, 2002]. There are no seasonal variations in tropospheric equilibrium temperature. In the stratosphere (above 200 hPa), the equilibrium temperature is set everywhere to those defined in the U.S. Standard Atmosphere (1976), except over the winter pole where a cold anomaly provides a representation of the stratospheric polar vortex. A simple seasonal cycle in equilibrium temperatures is prescribed in the stratosphere, such that the stratospheric equilibrium temperature at a given polar latitude varies between polar summer and polar winter over a 360 day year. Since there is no tropospheric seasonality in equilibrium temperature, any seasonal variations in the tropospheric circulation can be attributed unambiguously to the effects of stratospheric seasonality. The one difference from the setup of *Sheshadri et al.* [2015] is that here, we set the tropospheric asymmetry factor ε to a value of 10 K (i.e., the hemisphere analyzed is the "summer" hemisphere). The tropospheric asymmetry factor ε determines the annual mean tropospheric annular mode timescale (the decorrelation timescale of the principal component autocorrelation function associated with the first empirical orthogonal function (EOF) of zonal mean zonal wind [see, e.g., *Ring and Plumb*, 2008; *Gerber et al.*, 2008]), which is 28 days with ε set to 10 K. This avoids the problem of unrealistically large and persistent responses of the tropospheric jet to external forcings which was evident in *Polvani and Kushner* [2002], and also in the large seasonal drift of the tropospheric jet in certain experiments in *Sheshadri et al.* [2015]. The model configuration with no topography results in a Southern Hemisphere-like stratospheric seasonal variability in the model, with no stratospheric sudden warming events, and a final warming that occurs on the average on 10 December (about 3 weeks later than in the observations in the years prior to the development of the ozone hole). The climatology of the control run is very similar to the run without topography described in *Sheshadri et al.* [2015]. To this model setup, in order to mimic the radiative effects of stratospheric ozone depletion, we add diabatic cooling to the polar stratosphere (similar to that of *Butler et al.* [2010] and *Sun et al.* [2014] in the springtime distributed as follows:

$$Q(\phi,\sigma,t) = q_0 \exp\left[-\left\{\frac{(\phi-\phi_0)^2}{2\delta_\phi^2} + \frac{(-7000\ln\sigma + 7000\ln\sigma_0)^2}{2\delta_\sigma^2} + \frac{(t-t_0)^2}{2\delta_t^2}\right\}\right] \quad (1)$$

with $q_0 = -1$ K/d, $\phi_0 = -\frac{\pi}{2}$, $\delta_\phi = 0.28$, $\sigma_0 = 0.05$, $\delta_\sigma = 4000$, t_0 = Day 231, 261, 291, or 321 (corresponding to 20 August, 20 September, 20 October, and 20 November), $\delta_t = 20$ days, where ϕ_0, δ_ϕ, σ_0, and δ_σ define the spatial pattern and t_0 and δ_t define the peaking time and persistence. The choice of q_0 is such that the temperature changes in the stratosphere are about double what is evident in the observed stratosphere in the years with a large ozone hole. This change was made in order to enhance the statistical significance of

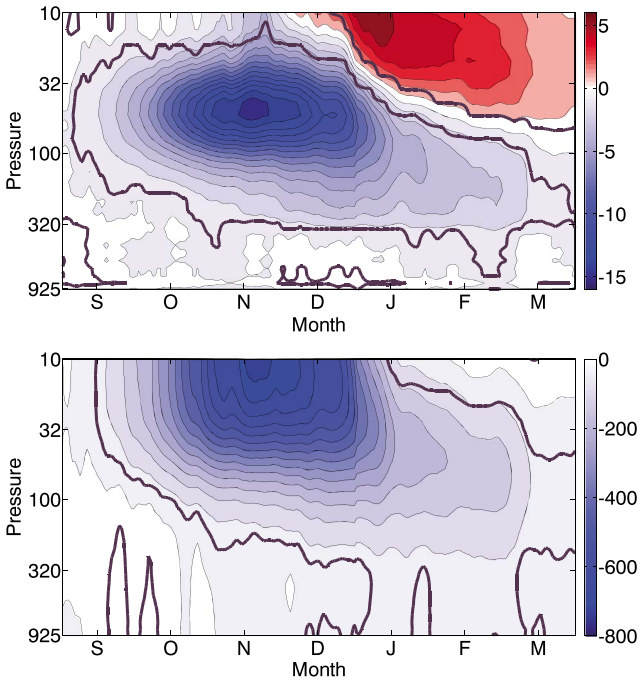

Figure 1. (top) Temperature response to the imposed polar stratospheric cooling averaged over the polar cap (65–90°S). The magenta contour denotes 95% statistical significance. The contour interval is 1 K. (bottom) Geopotential height changes averaged over the polar cap (65–90°S). The magenta contour denotes 95% statistical significance. The contour interval is 50 m.

the surface response. Additionally, a model integration was performed with steady (all-year) polar stratospheric cooling (i.e., simply removing the time dependent term in equation (1)), to examine the seasonality of tropospheric responses to a steady stratospheric cooling. The control run and the perturbed runs were all integrated for 35 years, and the last 30 years were analyzed.

3. Atmospheric Circulation Responses

3.1. Reference Case (October Cooling)

Figure 1 (top) shows the temperature changes evident in the model as a result of the imposed springtime polar stratospheric cooling. In addition to the expected statistically significant cooling that is evident in the lower stratosphere up to the end of January, a statistically significant warming above the cooling is evident above 30 hPa through the months of January, February, and March. This feature has been previously noted in both modeling and observational studies [*Calvo et al.*, 2012; *Young et al.*, 2013; *Keeble et al.*, 2014] as being of dynamical origin. It was attributed by *Calvo et al.* [2012] to the filtering of upward propagating gravity waves. However, since our model does not include a gravity wave parameterization, the existence of the warming-above-the-cooling feature must occur through changes in planetary-scale Rossby waves [as in *Yang et al.*, 2015]. As expected, the imposed lower stratospheric cooling also leads to an extension of the lifetime of the Antarctic vortex in the model, with the final warming being delayed by about two months in the perturbed run. Additionally, the standard deviation of the timing of final warming events increases (this is also evident in the observations, when the variability in the final warming date in the years with and without large ozone depletion is compared). The polar vortex strengthens, with wind anomalies extending downward into the troposphere in the summer. The corresponding changes in geopotential height averaged over the polar cap are shown in Figure 1 (bottom). The model's responses are qualitatively consistent with both observations and results from fully coupled chemistry climate models [cf. *Keeble et al.*, 2014]. Quantitatively, the imposed cooling leads to tropospheric changes in the model that are quite similar to observations of composite differences between the years of large ozone depletion and the preozone hole years [cf. *Thompson et al.*, 2011]. The model shows about a 50 m reduction in geopotential height at the surface over the polar cap, compared with a 40 m difference evident in Figure 1 of *Thompson et al.* [2011]. The surface changes extend well beyond polar latitudes. Statistically significant changes in the flux of wave activity into the stratosphere are also evident, with the eddy heat fluxes at 95 hPa showing an increase in magnitude and a poleward shift from mid-December through early March, consistent with the extended vortex lifetime (supporting information Figure S1).

The 850 hPa wind response is dipolar, with a strengthening/weakening of winds around 50°S/30°S. Although the wind response is predominantly dipolar throughout the period of December to March, the latitudinal structure of the wind changes matches the annular mode structure reasonably well only in February and March, being about 5° poleward of the annular mode peak in December and January (as shown in supporting information Figure S2). This is similar to the tropospheric response to stratospheric final warming events, which previous studies have established as differing in latitudinal structure from the leading mode both in observations [*Black et al.*, 2006; *Black and McDaniel*, 2007a, 2007b; *Hu et al.*, 2014] and in idealized models

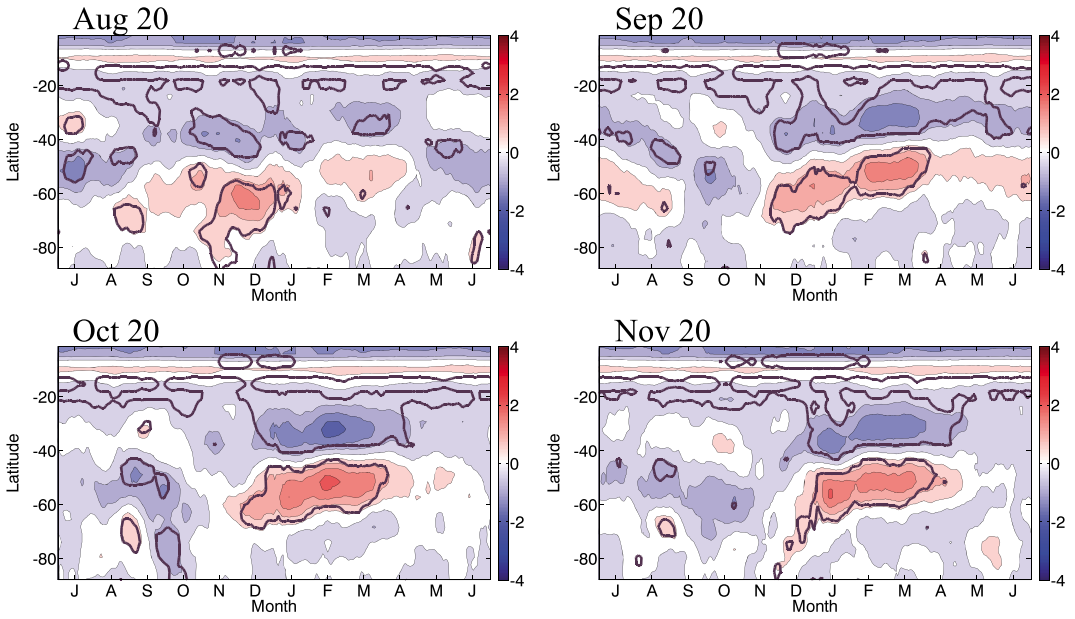

Figure 2. The 850 hPa zonal mean zonal wind response to polar stratospheric cooling that peaks (top row, left) 20 August, (top row, right) 20 September, (bottom row, left), 20 October, and (bottom row, right) 20 November. The magenta contour denotes 95% statistical significance. The contour interval is 0.5 m/s, and the ticks on the *x* axis indicate the middle of the month.

[*Sheshadri et al*., 2014], where the peak of the tropospheric response is almost 10° poleward of that of the leading annular mode. We will discuss this further in section 3.3.

3.2. Responses to Cooling at Different Times

Figure 2 shows the changes in 850 hPa winds (smoothed using a 21 day running mean) in the experiments with imposed polar stratospheric cooling that peaks on 20 August, 20 September, 20 October, and 20 November. With August cooling, the statistically significant response is confined to November, December, and early January. With September, October, and November cooling, the onset of the statistically significant near-surface response in winds is systematically delayed, with the onset moving from early December to mid-December and late December. However, the termination of the statistically significant surface response in all these cases occurs around the same time, from early to middle April. These results, which are very different from a simple surface dipole response that is merely shifted in time as the peak of the stratospheric cooling moves through the months, suggest that the background meteorology is important in setting the timing and persistence of surface responses at different times of the year (this, along with changes to the latitudinal structure of the response, is explored further in section 3.3).

When the imposed polar stratospheric cooling delays the lifetime of the polar vortex (the final warming), as it does by about two months in the case of the imposed cooling with a peak on 20 October, there are weak westerlies in the lower stratosphere for an additional period of time (December and January, during which easterlies were prevalent in the control run). In accordance with the Charney-Drazin condition [*Charney and Drazin*, 1961], this permits more persistent wave propagation into the stratosphere and extends the period during which lower stratospheric variability may be large. In other words, the "active" period during which the stratosphere and troposphere may couple is extended. In the case of the August cooling, the final warming is delayed into early January, which is also when the statistically significant surface response terminates. Therefore, we suggest that the delay in the final warming might play an important role in setting the surface response to ozone depletion, not because the surface response can be attributed to a delayed, otherwise unchanged, tropospheric response to the final warming itself, but simply because the presence of westerlies in the lower stratosphere extends the season of lower stratospheric variability.

3.3. Response to Steady (All-Year) Cooling

The experiment with cooling applied uniformly through the year, while unrealistic, proves to be quite informative about the characteristics of the near-surface wind response. The wind changes are the largest early in

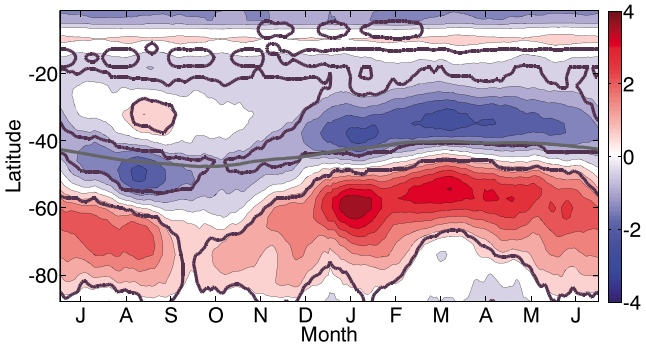

Figure 3. The 850 hPa zonal mean zonal wind response to polar stratospheric cooling all year round. The latitude of the jet maximum is shown in the grey curve. The magenta contour denotes 95% statistical significance. The contour interval is 0.5 m/s, and the ticks on the *x* axis indicate the middle of the month.

summer and autumn, with very much smaller responses in winter and, especially, early spring (Figure 3). This period of smaller responses coincides with a poleward shift of the mean jet (the latitude of maximum mean 850 hPa winds is shown in Figure 3 as a grey line) and a greater poleward drift of the maximum 850 hPa wind anomalies. Evidently, the tripolar structure of the response during summer does not reflect that of the dipolar annular mode. In fact, closer inspection shows this to be the case throughout the year; Figure 4 compares the mean 850 hPa wind response in January through May (JFMAM), when its structure is mostly dipolar, and in July through September (JAS), when it is more tripolar, with the structure of the two leading EOFs of zonal mean zonal wind. Even the dipolar response in JFMAM differs significantly from the dipolar EOF1, most notably in that the peaks of the response are displaced 5–10° poleward of the EOF. In JAS there is little correspondence between the two; in fact, they are almost in quadrature. Much of the discrepancy can be explained by an EOF2 component to the response. This second EOF is more tripolar than dipolar, it has a peak rather than a node near the mean wind maximum, and in this model it explains a substantial fraction of the variance in zonal mean wind, just as it does in Southern Hemisphere observations [e.g., *Lorenz and Hartmann*, 2001]. As Figure 4 shows, almost all the zonal wind response equatorward of 60°S can be explained as a sum of contributions from these two modes. At the highest latitudes, other modes are evidently contributing.

The responses in the case with cooling all through the year appear to be quite linear (a model experiment with half the forcing results in half the response with the same latitudinal structure, not shown). The fluctuation-dissipation theorem suggests that the response of any one mode to external forcings is proportional to the projection of the forcing onto the mode and to the mode timescale τ [e.g., *Ring and Plumb*, 2008; *Gerber et al.*, 2008]. Assessing the projection of the forcing involves specification of the coupling between the lower stratosphere and lower troposphere, which is still a matter of some uncertainty and beyond the scope of this paper. The role of the timescale can, however, be readily identified. We calculate τ as follows: we compute an autocorrelation function on a given day by using the principal component time series corresponding to the first (and second) EOF of zonal mean zonal wind for a period of 90 days centered on the day of interest. We average the autocorrelation function for that day of the year, from the 30 years of model data. We then calculate the decorrelation time of the average autocorrelation function as the best least squares fit to an exponential decay. Daily values of τ were smoothed using a centered 21 day moving average (similar to the smoothing applied to the 850 hPa wind changes in

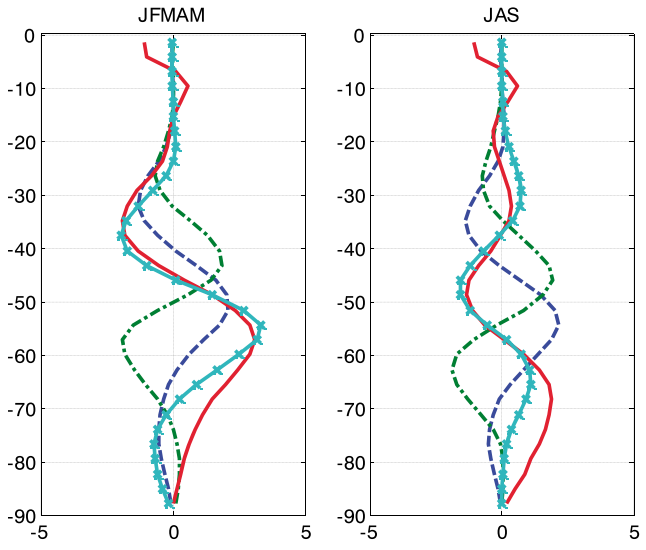

Figure 4. The 850 hPa wind responses from the case with all-year cooling averaged for the indicated months in the solid red curve, with the latitudinal structure of the first two EOFs shown using a blue dashed line and a green dash-dotted line, respectively. The sum of the parts of the response that are linearly dependent on EOFs 1 and 2 is shown in the cyan line.

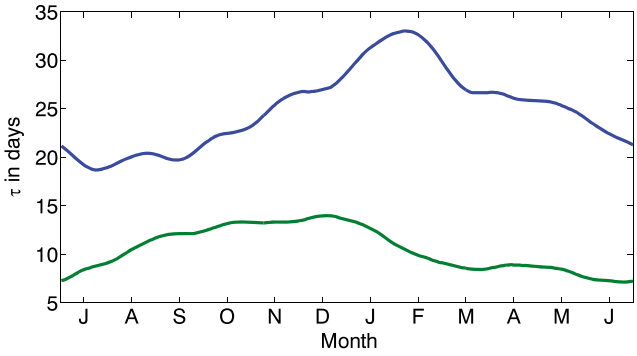

Figure 5. The seasonal cycle of the annular mode timescale (days) corresponding to EOFs 1 (blue line) and 2 (green line) of the control run at 850 hPa. The ticks on the *x* axis indicate the middle of the month.

Figures 2 and 3). Figure 5 shows the seasonality of 850 hPa τ for the two leading modes. We note that in our model setup, since the imposed seasonal cycle is confined to the stratosphere, all tropospheric seasonal changes (including the seasonality in the tropospheric τ) can be unambiguously attributed to coupling with the stratosphere. For EOF1, τ varies between minimum values of around 20 days in JAS to maximum values of around 30 days in JFM. Corresponding values for EOF2 range from around 10 days March through July up to about 15 days in October through January. Other things being equal, one would therefore anticipate that the response in mode 2, relative to mode 1, would vary by a factor of almost 2 over the course of the year, with mode 2 being relatively less important in January through July. This presumes that the projection of the forcing onto the modes does not change through the year; even though the imposed radiative forcing is fixed, its impact onto the tropospheric winds could vary seasonally.

4. Summary

When forced with a specified distribution of polar stratospheric cooling (meant to mimic the radiative impacts of stratospheric ozone depletion) that peaks in October (austral spring), the idealized model exhibits a tropospheric circulation response that is qualitatively consistent with the response to ozone depletion reported in studies involving both observations and comprehensive chemistry climate models. The imposed cooling leads to statistically significant temperature differences in the lower stratosphere, and to a strengthening of the polar vortex during the end of its lifetime in the control run. The delay of the final warming (the existence of westerlies at a time when easterlies were prevalent in the control run) permits planetary wave propagation into the stratosphere for a longer period of time. This is evident in the lower stratospheric heat fluxes, which show an increase through December, January, and February.

The model's surface responses to imposed polar stratospheric cooling are sensitive to the timing of the imposed cooling. When the imposed cooling is delayed from September to October to November, the onset of the statistically significant surface response is also delayed, but the termination of the response occurs at about the same time, suggesting the importance of the background meteorology at this time.

We suggest that when the imposed polar stratospheric cooling extends the lifetime of the polar vortex, this leads to an extension of the period of lower stratospheric variability during which the stratosphere and the troposphere may couple. This could be a factor in the responses of full general circulation models forced with specified ozone depletion. Specifically, if a model is forced with specified ozone concentrations inferred from observations, and the resulting stratospheric changes do not extend the lifetime of the Antarctic vortex in the model (which is entirely possible, since many models have a bias toward a final warming date that is too late in comparison to observations [e.g., *Butchart et al.*, 2011; *Wilcox and Charlton-Perez*, 2013]), the active season during which stratospheric variability could influence tropospheric circulation would not be extended. The idea that the extended vortex lifetime might be important, not because of the tropospheric response to the final warming but simply because of an extension of the period of lower stratospheric variability, is also consistent with the results of *Sun et al.* [2014] who reported that tropospheric wind trends consistent with observations are not evident in their model in years in which the final warming was not delayed.

The experiment with imposed cooling all year round revealed that the model's surface wind response cannot be described solely in terms of the leading EOF; rather, that EOFs 1 and 2 seem to be involved throughout the year, although in different proportions. This cautions against any assumption that the response of the atmosphere to external forcing can be described by a single "annular mode."

Acknowledgments
A.S. acknowledges support from the National Science Foundation through grant OCE-1338814. We thank Edwin Gerber, Diane Ivy, Bill Randel, Susan Solomon, and Lantao Sun for useful discussions. Numerical information is provided in the figures, and any additional data may be obtained from A.S. (email: as4915@columbia.edu). We are grateful to Lantao Sun and one anonymous reviewer for their helpful comments, which greatly improved the manuscript.

References

Archer, C. L., and K. Caldeira (2008), Historical trends in the jet streams, *Geophys. Res. Lett.*, *35*, L08803, doi:10.1029/2008GL033614.
Black, R. X., and B. A. McDaniel (2007a), The dynamics of Northern Hemisphere stratospheric final warming events, *J. Atmos. Sci.*, *64*, 2932–2946.
Black, R. X., and B. A. McDaniel (2007b), Interannual variability in the Southern Hemisphere circulation organized by stratospheric final warming events, *J. Atmos. Sci.*, *64*, 2968–2974.
Black, R. X., B. A. McDaniel, and W. A. Robinson (2006), Stratosphere–troposphere coupling during spring onset, *J. Clim.*, *19*, 4891–4901.
Butchart, N., et al. (2011), Multimodel climate and variability of the stratosphere, *J. Geophys. Res.*, *116*, D05102, doi:10.1029/2010JD014995.
Butler, A. H., D. W. J. Thompson, and R. Heikes (2010), The steady-state atmospheric circulation response to climate change—Like thermal forcings in a simple general circulation model, *J. Clim.*, *23*, 3474–3496.
Calvo, N., R. R. Garcia, D. R. Marsh, M. J. Mills, D. E. Kinnison, and P. J. Young (2012), Reconciling modeled and observed temperature trends over Antarctica, *Geophys. Res. Lett.*, *39*, L16803, doi:10.1029/2012GL052526.
Charney, J. G., and P. G. Drazin (1961), Propagation of planetary-scale disturbances from the lower into the upper atmosphere, *J. Geophys. Res.*, *66*, 83–109, doi:10.1029/JZ066i001p00083.
Fogt, R. L., J. Perlwitz, A. J. Monaghan, D. H. Bromwich, J. M. Jones, and J. G. Marshall (2009), Historical SAM variability. Part II: Twentieth-century variability and trends from reconstructions, observations, and the IPCC AR4 models, *J. Clim.*, *22*(20), 5346–5365.
Gerber, E. P., S. Voronin, and L. M. Polvani (2008), Testing the annular mode autocorrelation timescale in simple atmospheric general circulation models, *Mon. Weather Rev.*, *136*, 1523–1536.
Hu, J., R. Ren, Y. Yu, and H. Xu (2014), The boreal spring stratospheric final warming and its interannual and interdecadal variability, *Sci. China Ser. C.*, *57*, 710–718.
Hu, Y., and Q. Fu (2007), Observed poleward expansion of the Hadley circulation since 1979, *Atmos. Chem. Phys.*, *7*, 5229–5236.
Keeble, J., P. Braesicke, N. L. Abraham, H. K. Roscoe, and J. A. Pyle (2014), The impact of polar stratospheric ozone loss on Southern Hemisphere stratospheric circulation and climate, *Atmos. Chem. Phys.*, *14*, 13,705–13,717, doi:10.5194/acp-14-13705-2014.
Lorenz, D. J., and D. L. Hartmann (2001), Eddy–zonal flow feedback in the Southern Hemisphere, *J. Atmos. Sci.*, *58*, 3312–3327.
McLandress, C., T. G. Shepherd, J. F. Scinocca, D. A. Plummer, M. Sigmond, A. I. Jonsson, and M. C. Reader (2011), Separating the dynamical effects of climate change and ozone depletion. Part II: Southern Hemisphere troposphere, *J. Clim.*, *24*, 1850–1868.
Polvani, L. M., and P. J. Kushner (2002), Tropospheric response to stratospheric perturbations in a relatively simple general circulation model, *Geophys. Res. Lett.*, *29*(7), 1114, doi:10.1029/2001GL014284.
Polvani, L. M., D. W. Waugh, G. J. P. Correa, and S.-W. Son (2011), Stratospheric ozone depletion: The main driver of 20th Century atmospheric circulation changes in the Southern Hemisphere, *J. Clim.*, *24*, 795–812.
Previdi, M., and L. M. Polvani (2014), Climate system response to stratospheric ozone depletion and recovery, *Q. J. R. Meteorol. Soc.*, *140*, 2401–2419.
Ring, M. J., and R. A. Plumb (2008), The response of a simplified GCM to axisymmetric forcings: Applicability of the fluctuation-dissipation theorem, *J. Atmos. Sci.*, *65*, 3880–3898.
Sheshadri, A., R. A. Plumb, and D. I. V. Domeisen (2014), Can the delay in Antarctic polar vortex breakup explain recent trends in surface westerlies?, *J. Atmos. Sci.*, *71*, 566–573.
Sheshadri, A., R. A. Plumb, and E. P. Gerber (2015), Seasonal variability of the polar stratospheric vortex in an idealized AGCM with varying tropospheric wave forcing, *J. Atmos. Sci.*, *72*, 2248–2266.
Sigmond, M., and J. C. Fyfe (2014), The Antarctic sea ice response to the ozone hole in climate models, *J. Clim.*, *27*, 1336–1342.
Sigmond, M., J. C. Fyfe, and J. F. Scinocca (2010), Does the ocean impact the atmospheric response to stratospheric ozone depletion? *Geophys. Res. Lett.*, *37*, L12706, doi:10.1029/2010GL043773.
Sun, L., G. Chen, and W. A. Robinson (2014), The role of stratospheric polar vortex breakdown in Southern Hemisphere climate trends, *J. Atmos. Sci.*, *71*, 2335–2353.
Thompson, D. W. J., J. M. Wallace, and G. C. Hegerl (2000), Annular modes in the extratropical circulation: Part II: Trends, *J. Clim.*, *13*, 1018–1036.
Thompson, D. W. J., S. Solomon, P. J. Kushner, M. H. England, K. M. Grise, and D. J. Karoly (2011), Signatures of the Antarctic ozone hole in Southern Hemisphere surface climate change, *Nat. Geosci.*, *4*(11), 741–749.
Waugh, D. W., W. J. Randel, S. Pawson, P. A. Newman, and E. R. Nash (1999), Persistence of the lower stratospheric polar vortices, *J. Geophys. Res.*, *104*, 27,191–27,202, doi:10.1029/1999JD900795.
Wilcox, L., and A. J. Charlton-Perez (2013), Final warming of the Southern Hemisphere polar vortex in high- and low-top CMIP5 models, *J. Geophys. Res. Atmos.*, *118*, 2535–2546, doi:10.1002/jgrd.50254.
Yang, H., L. Sun, and G. Chen (2015), Separating the mechanisms of transient responses to stratospheric ozone depletion—Like cooling in an idealized atmospheric model, *J. Atmos. Sci.*, *72*, 763–773.
Young, P. J., A. H. Butler, N. Calvo, L. Haimberger, P. J. Kushner, D. R. Marsh, W. J. Randel, and K. H. Rosenlof (2013), Agreement in late twentieth century Southern Hemisphere stratospheric temperature trends in observations and CCMVal-2, CMIP3, and CMIP5 models, *J. Geophys. Res. Atmos.*, *118*, 605–613, doi:10.1002/jgrd.50126.